Journal of Young Pharmacists, 2026; 18(3):816-832.
https://www.jyoungpharm.org

Original Article

Network Pharmacology and Molecular Docking Analysis of *Amoora rohituka* Roxb. Reveals Bulnesol Modulates ESR1 and CYP2C19 Proteins as Potential Therapeutic Targets for Neuroprotection in the Management of Depression

Manjunatha Pai Chennaithody[1], Rajesh Kaverikana Shankar[1,*], Manappa T Mandalamari[2], Abdul Fairoz Ahamed[2]

[1]Nitte (Deemed to be University), NGSM Institute of Pharmaceutical Sciences (NGSMIPS), Department of Pharmacology, Mangalore, Karnataka, INDIA.
[2]Nitte (Deemed to be University), NGSM Institute of Pharmaceutical Sciences (NGSMIPS), Department of Pharmaceutical Chemistry, Mangalore, Karnataka, INDIA.

Correspondence:
Dr. Rajesh Kaverikana Shankar
Nitte (Deemed to be University), NGSM Institute of Pharmaceutical Sciences (NGSMIPS), Department of Pharmacology, Mangalore-575018, INDIA.
Email: rajeshks@nitte.edu.in

Received: 12-06-2026;
Revised: 28-07-2026;
Accepted: 03-09-2026.

ABSTRACT

Background: Depression is a multifactorial neuropsychiatric disorder involving multiple molecular targets and signalling pathways. *Amoora rohituka* has a variety of pharmacological properties but its antidepressant activity is still not explored. Hence, the antidepressant effect of *A. rohituka* was studied in an integrated systems pharmacology approach with a view to understanding the molecular mechanism behind it. **Materials and Methods:** The reported phytoconstituents from the leaves of *A. rohituka* were analysed for drug-likeness, pharmacokinetics, biological activity and adverse drug reactions through public databases. Network pharmacology, Gene Ontology, KEGG pathway enrichment, molecular docking and Prime MM-GBSA analysis were performed on common targets between phytoconstituents and depression. **Results:** 18 phytoconstituents were identified, out of which twelve were found to be having the drug-likeness properties. The results of network pharmacology revealed 132 common targets, among which MAPK1, AKT1, PARP1, CDK2 and GSK3β were the key proteins in the network hub. KEGG enrichment identified that significant pathways involved such as PI3K-Akt, MAPK, neurotrophin, serotonergic synapse, dopaminergic synapse, mTOR, TNF, NF-κB, JAK-STAT, AMPK and cAMP signalling pathways. Bulnesol, α-guaiene, himachalol, guaiol and β-eudesmol showed good molecular docking interactions with various depression-associated proteins. Bulnesol displayed the best docking scores for ESR1 (-8.20 kcal/mol) and CYP2C19 (-7.242 kcal/mol), and MM-GBSA analysis revealed low binding free energy and stable complexes. **Conclusion:** *Amoora rohituka* has potential antidepressant properties by coordinated modulation of depression associated proteins and signalling pathways. The results of the present study give mechanistic clues and suggest the phytoconstituents to be a promising source for further development of antidepressant drugs.

Keywords: *A. rohituka*, Bioactive, Docking, Network, Pathway, Protein.

INTRODUCTION

Depression is a widespread and crippling mental illness with symptoms of low mood, pessimism, and decreased interest or motivation that impacts emotional, cognitive and physical functioning (Stringaris, 2017). Symptoms include depressed mood, fatigue, sleep issues, decreased appetite, trouble concentrating, feelings of worthlessness, and even suicidal thoughts in extreme cases (Kumar *et al.*, 2012). Depression is a multifactorial disorder, including genetic vulnerability, neurotransmitter abnormalities, chronic stress, environmental factors, inflammatory mechanisms and neuroendocrine dysfunction (Brigitta, 2002). Pharmacotherapy, psychotherapy, and lifestyle changes are the main options for treatment. These interventions are effective, but they have a number of drawbacks, such as slow onset of action, partial symptom resolution, treatment resistance, relapse, and side effects such as weight gain, sexual dysfunction, gastrointestinal side effects, and sedation (Gumnick and Nemeroff, 2000). These drawbacks highlight the need for the development of safer and more effective therapeutic strategies for the management of depression. In the Indian traditional system of medicine, numerous medicinal herbs are used because of their high therapeutic potency with minimal adverse reactions. But the only challenge is its undiscovered mechanism of action, which is one of the causes of the lack of

DOI: 10.5530/jyp.20260347

medicinal utility (Chennaithody and Shankar, 2026). *Amoora rohituka* Roxb, also known as *Aphanamixis polystachya*, is an important medicinal plant belonging to the family Meliaceae and is widely distributed throughout India and other tropical regions of South and Southeast Asia. The plant has been extensively utilised in traditional systems of medicine for the treatment of various ailments such as liver disorders, splenomegaly, diabetes, inflammation, rheumatoid arthritis, gastrointestinal disorders, skin diseases, ulcers, helminthic infections, and tumours. Pharmacological investigations have demonstrated that extracts and isolated compounds from *A. rohituka* possess antioxidant, anti-inflammatory, antimicrobial, antidiabetic, hepatoprotective, immunomodulatory, neuroprotective, and anticancer activities, thereby supporting its traditional medicinal applications (Hossain *et al.*, 2023). Owing to its broad ethnomedicinal importance, *A. rohituka* has attracted considerable scientific attention, leading to the identification of numerous bioactive phytoconstituents, including alkaloids, limonoids, tetranortriterpenoids, flavonoids, glycosides, saponins, phytosterols, and terpenoids. Other reported compounds, such as aphanamixin, aphanamixinin, aphapolins A&B, aphananin, amoorinin, elemol, nerolidol, β-sitosterol, and various limonoid derivatives, further contribute to the therapeutic potential of the plant (Chennaithody, 2025). The rich phytochemical diversity and broad spectrum of biological activities exhibited by *A. rohituka* highlight its potential as a valuable source of therapeutic agents. But there is limited research exploring the significance of *A. rohituka* in the treatment of mental health disorders, including depression. In addition, the possible biological interactions, pathways and genes modulated via phytoconstituents from *A. rohituka* associated with depression have not been proven yet. Hence, the present study focussed to explore the possible proteins responsible for depression and also to predict the mechanism of action of *A. rohituka* in the management of depression through *in silico* tools.

MATERIALS AND METHODS

System biology

Mining of bioactive constituents and targets

A list of reported phytoconstituents of the leaf part of *A. rohituka* was retrieved from the Indian medicinal plants, Phytochemistry and Therapeutics (IMPPAT; https://cb.imsc.res.in/imppat/) database. The PubChem CID, molecular formula and molecular weight and canonical smiles were retrieved from the PubChem (https://pubchem.ncbi.nlm.nih.gov/) database. The targets of the individual phytoconstituents were retrieved from the SwissTargetPrediction database with a probability score>0 (http://www.swisstargetprediction.ch/) and DIGEP-Pred with Pa>0.9 (https://www.way2drug.com/digep-pred/). The targets involved in depression were retrieved from the database of Comparative Toxicogenomic Database (CTD) with an inference score≥150 (https://ctdbase.org/), Therapeutic Target Database (TTD) (https://idrblab.net/ttd/), Genecards with relevance score ≥7 (https://www.genecards.org/) and Online Mendelian Inheritance in Man (OMIM) database (https://www.omim.org/). Common targets between bioactives and depression were obtained through Venny (https://bioinfogp.cnb.csic.es/tools/venny/) databases (Dwivedi *et al.*, 2021a).

Drug likeness character, pharmacokinetic profile, biological activity, and Adverse Drug Reaction (ADR) of the bioactives

The drug likeness character and Blood-Brain Barrier (BBB) permeability score of the individual bioactives of the leaf part of *A. rohituka* were retrieved from MolSoft (https://molsoft.com/mprop/) by applying their SMILES (simplified molecular input line entry system). Only those bioactives whose Blood-Brain Barrier (BBB) permeability score≥2 and which follow the drug likeness character as per the Lipinski rule of five (Abraham and Myers, 2021) were taken for gene enrichment analysis and construction of a network, and the chemical structures were drawn using ChemDraw Pro 8.0 software (https://chemistrydocs.com/chemdraw-pro-8-0/). Further pharmacokinetic parameters, such as absorption, distribution, metabolism, excretion, toxicity, etc., of the individual phytoconstituents were predicted from ADMET LAB 2.0 (http://www.way2drug.com/ge/). Biological activity of phytoconstituents was predicted from PASS online (https://www.passonline.org/). ADR of the individual bioactives was predicted from the ADVERPred (https://www.way2drug.com/adverpred/) database (Dwivedi and Shastry, 2023).

Gene enrichment and network analysis

The identified common targets were subjected to the Search Tool for the Retrieval of Interacting Neighbouring Genes/Proteins (STRING) database (https://string-db.org/) to obtain protein-protein interaction, and KEGG) pathway. Moreover, to understand the pathways regulated by the proteins, the Kyoto Encyclopedia of Genes and Genomes (KEGG) pathway was retrieved, which was further connected to Cytoscape ver.3.10.3 to construct the network between compounds, targets, and pathways. The network was constructed based on "Degree". where parameters like centrality, neighbourhood connectivity, number of directed edges, radiality, etc. were obtained (Chaudhary *et al.*, 2022).

Gene ontology analysis

Gene Ontology (GO) provides a structured framework for the functional characterization of genes and gene products based on their associated Cellular Components (CC), Molecular Functions (MF), and Biological Processes (BP). The GO information for the selected genes was extracted from the STRING database to evaluate these functional categories (Dwivedi *et al.*, 2021b).

In silico molecular docking

Schrodinger Suite Glide was utilised for the molecular docking. The top 10 lead proteins identified from gene network analysis were used as targets, and leaf bioactives of *A. rohituka* that passed the drug likeness property were used as ligands for the molecular docking.

Ligand preparation

The two-Dimensional (2D) structures of the ligands were obtained from the PubChem database and imported into the computational workspace. These structures were subsequently converted into three-Dimensional (3D) models using the LigPrep module. Multiple ligand conformations were generated employing the OPLS-2005 force field, and the conformer exhibiting the lowest energy state was selected as the most stable structure. This optimised conformer was then utilised for subsequent molecular docking studies (Dwivedi *et al*., 2021b).

Selection and preparation of the target protein

The structures of the top 10 highly modulated proteins obtained from gene network construction were initially queried in the Universal Protein Resource (UniProt) database (*https://www.uniprot.org/*) and then queried in the Research Collaboratory for Structural Bioinformatics - Protein Data Bank (RCS PDB) database (RCSB; https://www.rcsb.org/). The protein structures were prepared using the Protein Preparation Wizard available in Schrödinger Maestro (Schrödinger, LLC, New York, NY, USA, 2021). During preparation, hydrogen atoms were added, crystallographic water molecules were removed, and partial atomic charges were assigned using the OPLS-2005 force field. Appropriate protonation states were generated, followed by restrained energy minimisation with an Root Mean Square Deviation (RMSD) cut-off of 0.3 Å to optimise the protein structure. Subsequently, the co-crystallised ligand was removed to identify the active site, and a receptor grid was generated with dimensions of 10 × 10 × 10 Å for molecular docking studies (Dwivedi *et al*., 2021). Table 1 summarises the list of selected protein targets and its respective standards.

Ligand-protein docking

Molecular docking of the individual bioactives was performed using the Glide module of the Schrödinger suite. Each ligand was docked into the predefined active site within the generated receptor grid. For every docking simulation, the binding pose exhibiting the lowest docking score was selected for further analysis. The ligand-protein interactions were subsequently visualised using the Glide XP Visualizer, and key interactions at the active site were examined alongside the corresponding docking scores to evaluate binding affinity and stability (Dwivedi *et al*., 2021b).

Binding free energy calculation (Prime MM-GBSA)

The binding free energies (ΔG_bind) of the protein-ligand complexes were further assessed using the Prime MM-GBSA method. This method integrates molecular mechanics energies with implicit solvation models to account for polar and non-polar solvation contributions. The obtained ΔG_bind values (kcal/mol) served as indicators of binding strength and complex stability, thereby enhancing reliability in the virtual screening outcomes (Fathima *et al*., 2026).

RESULTS

System biology

Mining of bioactive constituents and targets

A total of 18 leaf bioactive compounds were identified in *A. rohituka*. Table 2 summarizes the list of bioactives along with their PubChem CIDs, molecular formulas, and molecular weights. The chemical structures of the individual bioactives were drawn in Figure 1. A total of 1,540 targets (70.7%), as predicted by SwissTargetPrediction and DIGEP-Pred, were associated with the bioactives. For depression, 638 targets (23.2%) were identified from the CTD, TTD, GeneCards, and OMIM databases. Venny analysis revealed 132 common targets shared between the bioactives and depression (Figure 2 and Supplementary file 1 (sheet 1-3)).

Drug likeness character, pharmacokinetic profile, biological activity, and Adverse Drug Reaction (ADR) of the bioactives

According to the Molsoft database, 12 out of the 18 leaf phytoconstituents of *A. rohituka* complied with the drug-likeness criteria based on Lipinski's Rule of Five. Six bioactives, namely geranylgeraniol, β-elemene, humulene, phytol, β-sitosterol, and β-selinene, were found to violate one or more of the drug-likeness criteria. Therefore, only these 12 phytomolecules were selected for gene enrichment, gene Ontology, and network analyses. Among the selected compounds, himachalol, α-eudesmol, β-eudesmol, and γ-eudesmol exhibited the highest Blood-Brain Barrier (BBB) permeability score of 4.39. Germacrene A, guaiol, bulnesol, caryophyllene oxide, and β-caryophyllene showed the highest drug-likeness score of 0.29, as predicted by the Molsoft database (Table 3). According to the SwissADME database, himachalol, α-panasinsene, humulene, caryophyllene oxide, and β-caryophyllene possessed no rotatable bonds (Figure 3 and Supplementary File 2). α-guaiene had a Probability of Activity (Pa) value of 0.334 as a 5-HT release stimulant. Himachalol exhibited a Pa value of 0.228 for dopamine release stimulation, while γ-eudesmol showed a Pa value of 0.432 as a neurotransmitter uptake inhibitor (Table 4). Furthermore, 15 of the reported leaf bioactives of *A. rohituka* were predicted to be free from adverse effects according to the AdverPred database (Table 5).

Table 1: Selected proteins and reference standard for molecular docking.

Sl. No.	PDB ID	Protein	Reference standard
01.	1TVO	Mitogen-Activated Protein Kinase 1 (MAPK1)	Erlotinib
02.	IUNQ	AKT Serine/Threonine Kinase 1 (AKT1)	Fluvestrant
03.	1S9J	Mitogen-Activated Protein Kinase 1(MAP2K1)	Trametinib
04.	7Y5X	Presenilin 2 (PSEN2)	Nirogacestat
05.	5I71	Solute Carrier Family 6 Member 4 (SLC6A4)	Citalopram
06.	2P54	Peroxisome Proliferator-Activated Receptor Alpha (PPARA)	Fenofibrate
07.	3LDQ	Heat Shock Protein Family A Member 8 (HSPA8)	Acetaminophen
08.	3SWZ	Cytochrome P450 Family 17 Subfamily A Member 1 (CYP17A1)	Ketoconazole
09.	1XPC	Estrogen Receptor 1 (ESR1)	Tamoxifen
10.	4GQS	Cytochrome P450 Family 2 Subfamily C Member 19 (CYP2C19)	Doxepin

Gene enrichment and Network analysis

The common targets shared between the bioactives and depression were analysed using the STRING database to evaluate Protein-Protein Interactions (PPIs) (Figure 4). A total of 189 KEGG-integrated pathways were identified, of which 15 were found to be closely associated with the pathogenesis and management of depression (Table 6). The integrated bioactive-protein-pathway network was constructed and analysed using Cytoscape software, and the network components were ranked based on their edge counts (Figure 5). Among the identified pathways, the PI3K-Akt signalling pathway (KEGG ID: hsa04151) emerged as the most prominently modulated pathway within the network, with an observed gene count of 349, a strength score of 0.90, a signal score of 1.67, an edge count of 17, an eccentricity of 6, a neighborhood connectivity of 4.5, a radiality of 0.95, and a closeness centrality of 0.34 (Supplementary File 3). Himachalol was identified as the lead bioactive compound in the network, exhibiting an edge count of 39, an eccentricity of 5, a neighborhood connectivity of 4.46, a radiality of 0.90, and a closeness centrality of 0.39. Similarly, MAPK1 was identified as the key protein in the network, with an edge count of 14, an eccentricity of 5, a neighborhood connectivity of 16.5, a radiality of 0.96, and a closeness centrality of 0.43.

Gene ontology

The identified targets were functionally characterised using Gene Ontology (GO) analysis, and the corresponding Cellular Component (CC), Molecular Function (MF), and Biological Process (BP) annotations were extracted from the STRING database. GO analysis identified 97 CC in which 'intracellular anatomical structure' (GO:0005622) scored the lowest False Discovery Rate (FDR) of 8.10E-05 by the modulation of 123 genes. Similarly, 92 MF were identified in which 'signalling receptor binding' (GO:0005102) scored the lowest FDR of 9.71E-06 with the modulation of 31 genes. Moreover, 1337 BP were identified in which 'regulation of multicellular organismal process' (GO:0051239) scored the lowest FDR of 9.8E-32 with the modulation of 81 genes (Supplementary File 4 (sheet 1-3)).

Molecular docking

Molecular docking analysis demonstrated favourable binding interactions between the selected phytoconstituents and their respective depression-associated protein targets. Among the identified compounds, bulnesol exhibited the strongest and broadest binding profile, showing affinity towards estrogen receptor 1 (ESR1; PDB ID: 1XPC), cytochrome P450 family 2 subfamily C member 19 (CYP2C19; PDB ID: 4GQS), cytochrome P450 family 2 subfamily C member 9 (CYP2C9; PDB ID: 3SWZ), epidermal growth factor receptor (EGFR; PDB ID: 1TV0), cyclin-dependent kinase 2 (CDK2; PDB ID: 3LDQ), and estrogen-related receptor gamma (ESRRG; PDB ID: 1UNQ), with docking scores of -8.20, -7.242, -6.932, -5.746, -5.052, and -4.049 kcal/mol, respectively. Against ESR1, bulnesol formed hydrophobic interactions with ILE31, LEU156, MET108, LEU107, VAL39, ALA52, ILE84, and CYS166, together with polar interactions involving SER153, THR110, and GLN105, while GLN105 formed a hydrogen bond. In CYP2C19, hydrophobic interactions were observed with ALA106, ILE205, VAL208, ALA103, LEU102, PHE114, PHE100, VAL113, PHE476, LEU366, ALA297, ALA292, LEU201, MET240, LEU237, and LEU233, whereas ASN107 and ASN204 participated in both polar interactions and hydrogen bond formation. Binding to CYP2C9 involved hydrophobic contacts with TYR201, ILE205, ILE206, VAL482, VAL483, LEU209, ALA105, PHE114, and ALA113, along with polar interactions with SER106 and ASN202. Similar interactions were observed with EGFR, where hydrophobic interactions occurred with ILE31, LEU156, MET108, LEU107, VAL39, ALA52, ILE84, and CYS166, accompanied by polar interactions involving SER153, THR110, and GLN105 and a hydrogen bond with GLN105. In CDK2, bulnesol interacted hydrophobically with ILE343, while SER275 and SER340 formed polar interactions and GLU231 and LYS271 participated in hydrogen bonding. Against ESRRG, hydrophobic interactions were observed with

LEU52, PHE55, and TYR18, polar interactions with ASN54, ASN53, and TYR18, and hydrogen bonds involving LEU52 and ASN53.α-Guaiene exhibited favourable binding towards peroxisome proliferator-activated receptor alpha (PPARA; PDB ID: 2P54) with a docking score of -7.008 kcal/mol. The ligand established hydrophobic interactions with ALA250, ILE241, PHE343, LEU344, LEU247, ILE272, ILE339, CYS275, CYS276, MET330, VAL332, ALA333, LEU258, VAL255, and LEU254, together with a polar interaction involving THR279. Himachalol demonstrated favourable binding towards solute carrier family 6 member 4 (SLC6A4; PDB ID: 5I71) with a docking score of -6.980 kcal/mol through hydrophobic interactions with TYR18, ILE19, and PHE55, a polar interaction with ASN53, and a hydrogen bond with GLU17. Guaiol exhibited a docking score of -6.276 kcal/mol against mitogen-activated protein kinase 1 (MAPK1; PDB ID: 1S9J), forming hydrophobic contacts with MET219, ILE216, LEU215, LEU115, LEU118, VAL211, ILE141, PHE209, and ILE99, polar interactions with SER212 and ASN192, and a hydrogen bond with PHE209. β-Eudesmol demonstrated binding towards presenilin 2 (PSEN2; PDB ID: 7Y5X) with a docking score of -4.029 kcal/mol by forming hydrophobic interactions with ALA700, ILE699, PHE698, and ALA694, a polar interaction with ASN691, and a hydrogen bond with PHE698. The docking performance of the phytoconstituents was compared with their respective reference ligands. Tamoxifen exhibited the highest binding affinity towards ESR1 (-9.985 kcal/mol), followed by ketoconazole towards CYP2C9 (-8.965 kcal/mol), fenofibrate towards PPARA (-8.814 kcal/mol), citalopram towards SLC6A4 (-7.841 kcal/mol), trametinib towards MAPK1 (-7.709 kcal/mol), doxepin towards CYP2C19 (-7.329 kcal/mol), acetaminophen towards CDK2 (-5.120 kcal/mol), erlotinib towards EGFR (-5.054 kcal/mol), fulvestrant towards ESRRG (-3.444 kcal/mol), and nirogacestat towards PSEN2 (-1.975 kcal/mol).Overall, the selected phytoconstituents demonstrated favourable binding orientations within the active sites of the target proteins through combinations of hydrophobic contacts, polar interactions, and hydrogen bonds, supporting their predicted affinity towards multiple depression-associated molecular targets (Table 7). Two-Dimensional (2D) and Three-Dimensional (3D) images of the top 3 ligands with high binding affinity has been represented in Figures 6-8.

Binding free energy calculation (Prime MM-GBSA)

Molecular Mechanics Generalised Born Surface Area (MM-GBSA) analysis was performed to determine the binding free energy and its individual energy components for the ligand-protein complexes. Bulnesol against 1XPC exhibited a binding free energy (ΔG bind) value of -42.18 kcal/mol, with Coulomb energy (ΔG Coulomb), covalent energy (ΔG Covalent), lipophilic energy (ΔG Lipo), solvation energy (ΔG Solv GB), and van der Waals energy (ΔG vdW) values of -3.03, 5.08, -25.07, 13.58, and -31.97 kcal/mol, respectively. Against 4GQS, bulnesol

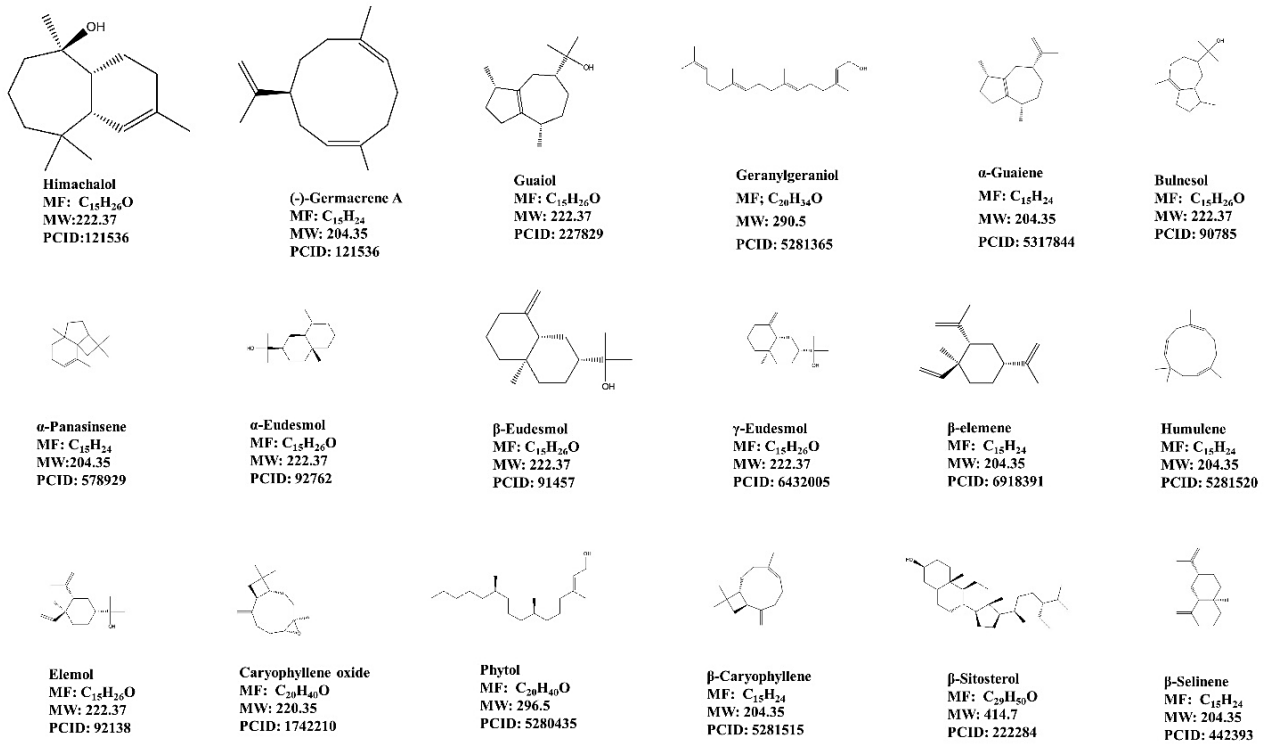

Figure 1: Chemical structure of the reported leaf phytoconstituents of the *A. rohituka.*

Table 2: Reported bioactives from *A. rohituka*.

Sl. No.	Bioactives	PubChem CID	Molecular formula	Molecular weight
01.	Himachalol	121536	$C_{15}H_{26}O$	222.37
02.	(-)-Germacrene A	9548706	$C_{15}H_{24}$	204.35
03.	Guaiol	227829	$C_{15}H_{26}O$	222.37
04.	Geranylgeraniol	5281365	$C_{20}H_{34}O$	290.5
05.	Alpha-Guaiene	5317844	$C_{15}H_{24}$	204.35
06.	Bulnesol	90785	$C_{15}H_{26}O$	222.37
07.	Beta-elemene	6918391	$C_{15}H_{24}$	204.35
08.	Alpha-Panasinsene	578929	$C_{15}H_{24}$	204.35
09.	Alpha-Eudesmol	92762	$C_{15}H_{26}O$	222.37
10.	Beta-Eudesmol	91457	$C_{15}H_{26}O$	222.37
11.	Gamma-Eudesmol	6432005	$C_{15}H_{26}O$	222.37
12.	Humulene	5281520	$C_{15}H_{24}$	204.35
13.	Elemol	92138	$C_{15}H_{26}O$	222.37
14.	Caryophyllene oxide	1742210	$C_{20}H_{40}O$	220.35
15.	Phytol	5280435	$C_{20}H_{40}O$	296.5
16.	Beta-Caryophyllene	5281515	$C_{15}H_{24}$	204.35
17.	Beta-Sitosterol	222284	$C_{29}H_{50}O$	414.7
18.	Beta-Selinene	442393	$C_{15}H_{24}$	204.35

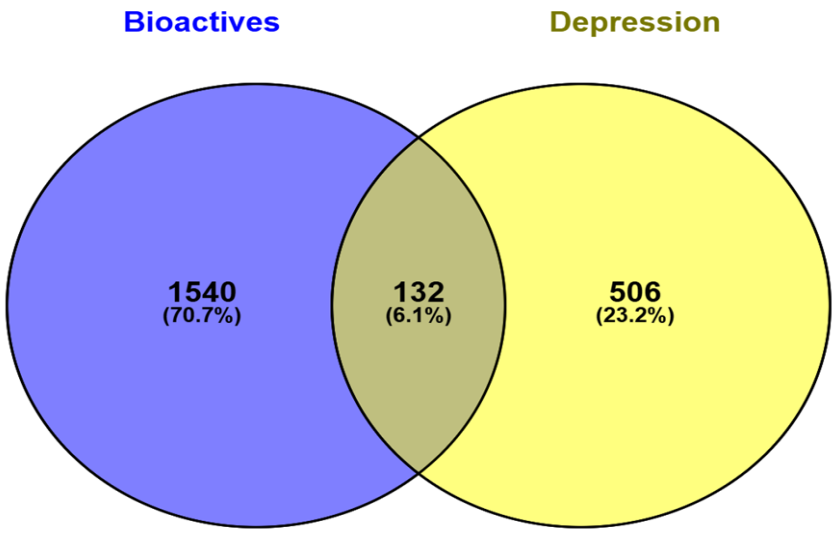

Figure 2: Venn diagram representation of (a) targets involved in bioactives vs targets involved in depression.

showed a ΔG bind value of -43.66 kcal/mol with corresponding ΔG Coulomb, ΔG Covalent, ΔG Lipo, ΔG Solv GB, and ΔG vdW values of -10.72, 1.92, -19.35, 14.41, and -29.40 kcal/mol, respectively. α-guaine against 2P54 exhibited a ΔG bind value of -34.37 kcal/mol, with ΔG Coulomb, ΔG Covalent, ΔG Lipo, ΔG Solv GB, and ΔG vdW values of -44.46, -1.77, -24.76, 6.82, and -20.69 kcal/mol, respectively. Himachalol against 5I71 showed a ΔG bind value of -17.95 kcal/mol with corresponding ΔG Coulomb, ΔG Covalent, ΔG Lipo, ΔG Solv GB, and ΔG vdW values of -8.93, 2.10, -18.99, 42.21, and -33.80 kcal/mol, respectively. Bulnesol further exhibited ΔG bind values of -31.41, -29.20, -22.35, and -25.21 kcal/mol against 3SWZ, 1TV0, 3LDQ, and 1UNQ, respectively, while guaiol against 1S9J and β-eudesmol against 7Y5X demonstrated ΔG bind values of -26.94 and -42.40 kcal/mol, respectively.The standard compounds exhibited ΔG bind values of -70.98 kcal/mol for tamoxifen against

1XPC, -43.14 kcal/mol for doxepin against 4GQS, -52.14 kcal/mol for fenofibrate against 2P54, -22.73 kcal/mol for citalopram against 5I71, -54.35 kcal/mol for ketoconazole against 3SWZ, -79.22 kcal/mol for trametinib against 1S9J, -33.87 kcal/mol for erlotinib against 1TV0, -24.24 kcal/mol for acetaminophen against 3LDQ, -42.40 kcal/mol for nirogastat against 1UNQ, and -26.81 kcal/mol for fluvestrant against 7Y5X. The corresponding ΔG Coulomb, ΔG Covalent, ΔG Lipo, ΔG Solv GB, and ΔG vdW values are presented in Table 8.

DISCUSSION

Depression is a complex neuropsychiatric disorder involving dysregulation of multiple neurotransmitter systems, neuroinflammation, oxidative stress, impaired neuroplasticity, and abnormalities in intracellular signalling pathways. Consequently, the conventional one-drug-one-target approach often fails to provide complete therapeutic benefit, highlighting the need for multitarget therapeutic strategies. Plant-derived bioactive compounds possess the ability to simultaneously regulate multiple proteins and signalling pathways, making them promising candidates for the management of multifactorial disorders such as depression. In the present study, a systems pharmacology approach integrating network pharmacology, molecular docking, and Molecular Mechanics Generalised Born Surface Area (MM-GBSA) analysis was employed to elucidate the possible molecular mechanisms underlying the antidepressant potential of *Amoora rohituka*. The present investigation identified eighteen reported leaf bioactives from *A. rohituka*, of which twelve fulfilled the drug-likeness criteria based on Lipinski's Rule of Five and therefore were considered suitable for further computational analyses. Drug-likeness screening is an essential initial step in natural product-based drug discovery because bioactives possessing favourable physicochemical characteristics are more likely to exhibit acceptable pharmacokinetic behaviour and oral bioavailability. Moreover, several selected compounds, particularly himachalol and the eudesmol isomers, demonstrated high predicted blood-brain barrier permeability, suggesting their capability to reach the central nervous system, an essential

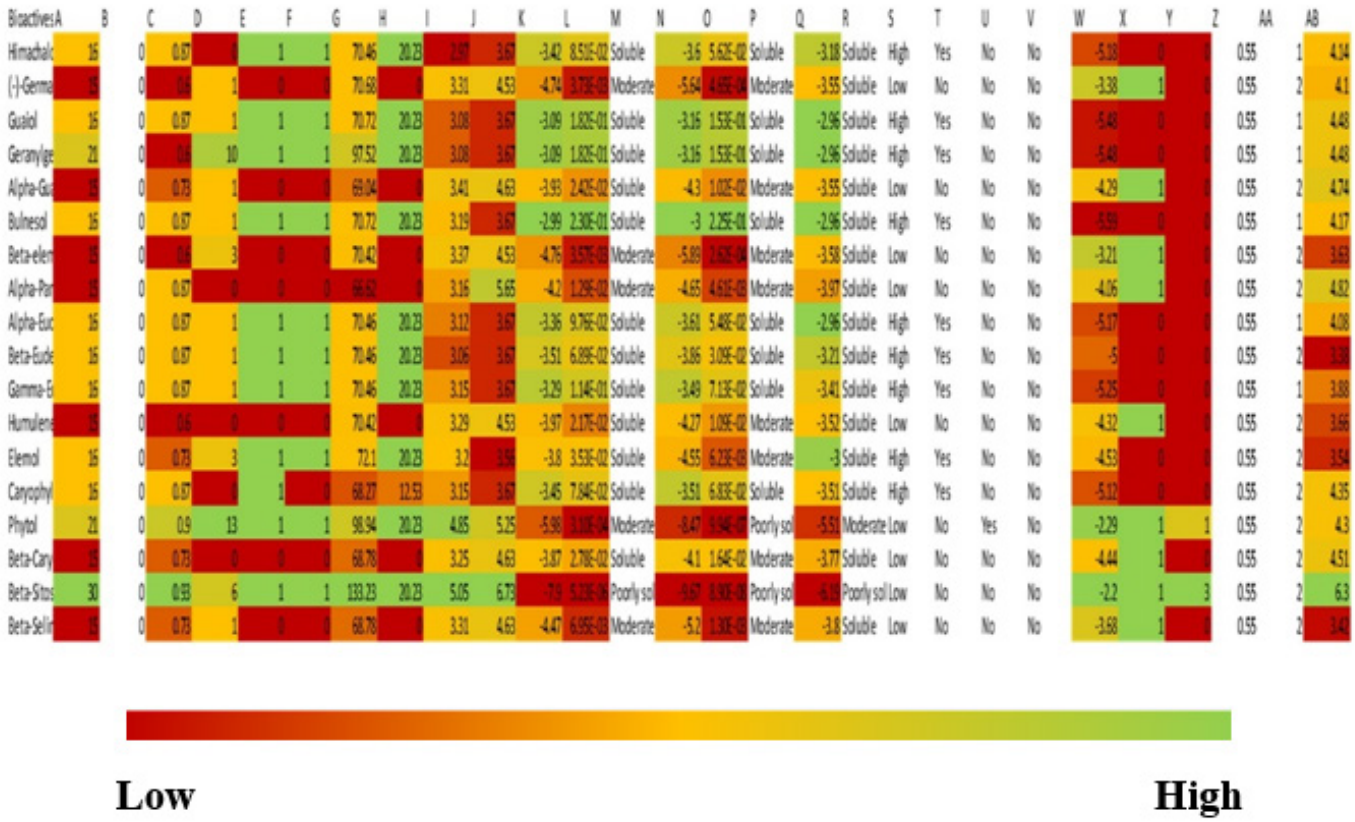

Figure 3: Heatmap presenting the ADMET profile of leaf phytomolecules of *A.rohituka.* (A) Number of Heavy Atoms, (B) Number of Aromatic Heavy Atoms, (C) Fraction of Carbon Atoms with sp^3 Hybridization (Fraction Csp^3), (D) Number of Rotatable Bonds, (E) Number of Hydrogen Bond Acceptors (HBA), (F) Number of Hydrogen Bond Donors (HBD), (G) Molar Refractivity (MR), (H) Topological Polar Surface Area (TPSA), (I) Intrinsic Logarithm of the Octanol/Water Partition Coefficient (iLOGP), (J) Moriguchi Logarithm of the Octanol/Water Partition Coefficient (MLOGP), (K) Estimated Solubility Logarithm (ESOL Log S), (L) Estimated Solubility by the ESOL Model (mg/mL), (M) ESOL Solubility Class, (N) Ali Model Predicted Solubility Logarithm (Ali Log S), (O) Predicted Solubility by the Ali Model (mg/mL), (P) Ali Solubility Class, (Q) Silicos-IT Predicted Aqueous Solubility Logarithm (Silicos-IT LogSw), (R) Silicos-IT Solubility Class, (S) Gastrointestinal Absorption (GI Absorption), (T) Blood-Brain Barrier Permeability (BBB Permeant), (U) P-glycoprotein (P-gp) Substrate, (V) Cytochrome P450 1A2 (CYP1A2) Inhibitor, (W) Logarithm of the Skin Permeation Coefficient (log Kp, cm/s), (X) Number of Violations of Lipinski's Rule of Five, (Y) Number of Violations of the Ghose Filter, (Z) Oral Bioavailability Score, (AA) Number of Violations of Lead-likeness Criteria, (AB) Synthetic Accessibility Score.

Table 3: The drug likeness characteristics of phytomolecules from *A. rohituka*.

Sl.No.	Phytomolecules	MF	MW	NHBA	NHBD	MolLogP	MolLogS		BBB	DLS
							Log(moles/L)	mg/L		
01.	Himachalol	$C_{15}H_{26}O$	222.37	1	1	4.24	-4.56	6.15	4.39	-0.85
02.	(-)-Germacrene A	$C_{15}H_{24}$	204.35	3	1	2.68	-2.84	375.19	4.25	0.29
03.	Guaiol	$C_{15}H_{26}O$	222.37	3	1	2.68	-2.84	375.19	4.25	0.29
04.	Geranylgeraniol	$C_{20}H_{34}O$	290.5	1	1	7.61	-6.01	0.28	4.32	-1.17
05.	Alpha-Guaiene	$C_{15}H_{24}$	204.35	0	0	4.93	-4.73	3.83	1.26	-1.24
06.	Bulnesol	$C_{15}H_{26}O$	222.37	3	1	2.68	-2.84	375.19	4.25	0.29
07.	Beta-elemene	$C_{15}H_{24}$	204.35	0	0	5.84	-5.67	0.43	1.26	-1.15
08.	Alpha-Panasinsene	$C_{15}H_{24}$	204.35	0	0	4.63	-4.31	9.98	1.26	-0.94
09.	Alpha-Eudesmol	$C_{15}H_{26}O$	222.37	1	1	4.36	-4.08	18.34	4.39	-0.47
10.	Beta-Eudesmol	$C_{15}H_{26}O$	222.37	1	1	4.37	-4.18	14.77	4.39	-0.60
11.	Gamma-Eudesmol	$C_{15}H_{26}O$	222.37	1	1	4.25	-4.17	15.07	4.39	0.02
12.	Humulene	$C_{15}H_{24}$	204.35	0	0	6.23	-5.77	0.35	1.26	-1.42
13.	Elemol	$C_{15}H_{26}O$	222.37	1	1	4.62	-4.20	13.95	4.39	-0.91
14.	Caryophyllene oxide	$C_{20}H_{40}O$	220.35	1	0	3.97	-4.30	11.05	4.25	0.29
15.	Phytol	$C_{20}H_{40}O$	296.5	1	1	7.72	-5.99	0.30	4.31	-0.87
16.	Beta-Caryophyllene	$C_{15}H_{24}$	204.35	3	1	2.68	-2.84	375.19	4.25	0.29
17.	Beta-Sitosterol	$C_{29}H_{50}O$	414.7	1	1	8.45	-6.34	0.19	3.94	0.78
18.	Beta-Selinene	$C_{15}H_{24}$	204.35	0	0	5.60	-5.35	0.92	1.26	-0.64

MF: Molecular Formula, MW: Molecular weight (g/mol), NHBA: Number of Hydrogen Bond Acceptors, NHBD: Number of Hydrogen Bond Donors, BBB: Blood Brain Barrier, DLS: Drug Likeliness Score.

prerequisite for antidepressant activity. The absence of predicted major adverse drug reactions for most of the selected bioactives further supports their potential safety profile. Although these predictions require experimental confirmation, they provide preliminary evidence that *A. rohituka* contains phytoconstituents with favourable pharmacological characteristics suitable for central nervous system drug development. PASS prediction further supported the potential neuropharmacological activity of these compounds. Himachalol demonstrated predicted neurotrophic factor enhancement and dopamine release stimulation, whereas α-guaiene showed predicted 5-hydroxytryptamine release stimulatory activity. Similarly, γ-eudesmol, β-eudesmol, elemol, caryophyllene oxide and β-caryophyllene were predicted to inhibit neurotransmitter uptake, while α-eudesmol and β-caryophyllene exhibited predicted γ-aminobutyric acid aminotransferase inhibitory activity. Several phytoconstituents also demonstrated predicted modulation of Mitogen-Activated Protein Kinase (MAPK), Janus Kinase 2 (JAK2), Cyclic Adenosine Monophosphate (cAMP), Nuclear Factor Erythroid 2-Related Factor 2 (Nrf2), and nitric oxide synthase signalling, indicating that *A. rohituka* may regulate multiple biological processes associated with depression rather than acting exclusively through monoamine neurotransmission. These observations agree with the current understanding that effective antidepressant therapies often exert pleiotropic actions involving neurotransmission, neuroplasticity, oxidative stress regulation, and inflammatory signalling. Network pharmacology identified 132 common targets shared between the phytoconstituents of *A. rohituka* and depression, demonstrating the multitarget nature of the plant. Protein-protein interaction analysis further revealed extensive interactions among these proteins, indicating coordinated regulation of several biological processes implicated in depression. Network topology identified MAPK1 as one of the principal hub proteins, while himachalol emerged as the most highly connected phytoconstituent within the bioactive-target-pathway network. Hub proteins generally exert greater regulatory influence because they interact with numerous signalling molecules, suggesting that modulation of MAPK1 and its associated signalling cascade may contribute substantially to the predicted antidepressant activity of *A. rohituka* (Hopkins, 2008; Barabási *et al.*, 2011). Among the enriched pathways, the Phosphoinositide 3-Kinase-Protein Kinase B (PI3K-Akt) signalling pathway demonstrated the greatest network connectivity. Dysregulation of PI3K-Akt signalling has been extensively implicated in depression owing to its essential role in neuronal survival, synaptic plasticity, neurogenesis, and regulation of apoptosis (Duman *et al.*, 2016; Kitagishi *et al.*, 2012). Activation of this pathway promotes phosphorylation of downstream proteins, including Glycogen Synthase Kinase-3 Beta (GSK3β), Mammalian Target of

Rapamycin (mTOR), and B-Cell Lymphoma 2 (BCL2), thereby enhancing neuronal survival and neuroplasticity (Kitagishi *et al.*, 2012; Beurel *et al.*, 2015). Previous studies have demonstrated that several clinically effective antidepressants partially restore impaired PI3K-Akt signalling, resulting in increased brain-derived neurotrophic factor expression and improved synaptic function (Duman and Aghajanian, 2012; Castrén and Monteggia, 2021). Therefore, the prominent enrichment of this pathway suggests that modulation of PI3K-Akt signalling may represent one of the principal molecular mechanisms through which *A. rohituka* exerts antidepressant activity. The mitogen-activated protein kinase signalling pathway also demonstrated high enrichment within the present study. MAPK signalling regulates neuronal differentiation, learning, memory, cellular survival, inflammatory responses, and neuroplasticity (Thomas and Huganir, 2004; Cargnello and Roux, 2011). Chronic stress and depressive disorders are associated with abnormal MAPK activation, ultimately leading to impaired neuronal function and reduced synaptic connectivity (Duric *et al.*, 2010; Duman *et al.*, 2016). The identification of MAPK1 and MAP2K1 as highly connected proteins suggests that modulation of this pathway may contribute to the restoration of neuronal signalling and synaptic adaptation. Consistent with these findings, PASS prediction also identified MAP kinase stimulatory activity for guaiol, bulnesol and α-eudesmol, further supporting the potential involvement of MAPK signalling in the pharmacological action

Table 4: The biological spectra of phytomolecules from *A. rohituka* against depression.

Sl. No.	Phytomolecules	Pa	Pi	Activity
01.	Himachalol	0,313	0,012	Neurotrophic factor enhancer
		0,228	0,076	Dopamine release stimulant
02.	(-)-Germacrene A	0,506	0,005	NF-E2-related factor 2 (Nrf2) stimulant
		0,598	0,004	NOS2 expression inhibitor
03.	Guaiol	0,465	0,057	MAP kinase stimulant
		0,468	0,062	JAK2 expression inhibitor
04.	Alpha-Guaiene	0,334	0,096	5 Hydroxytryptamine release stimulant
		0,338	0,124	Cyclic AMP agonist
05.	Bulnesol	0,361	0,119	MAP kinase stimulant
		0,350	0,108	JAK2 expression inhibitor
06.	Alpha-Panasinsene	0,738	0,002	NF-E2-related factor 2 stimulant
		0,715	0,016	JAK2 expression inhibitor
07.	Alpha-Eudesmol	0,354	0,129	MAP kinase stimulant
		0,310	0,106	GABA aminotransferase inhibitor
08.	Beta-Eudesmol	0,461	0,010	MAP3K5 inhibitor
		0,427	0,097	Neurotransmitter uptake inhibitor
09.	Gamma-Eudesmol	0,432	0,094	Neurotransmitter uptake inhibitor
		0,414	0,080	JAK2 expression inhibitor
10.	Elemol	0,315	0,098	Cyclic AMP agonist
		0,301	0,123	Neurotransmitter uptake inhibitor
11.	Caryophyllene oxide	0,340	0,114	JAK2 expression inhibitor
		0,323	0,198	Neurotransmitter uptake inhibitor
12.	Beta-Caryophyllene	0,387	0,151	Neurotransmitter uptake inhibitor
		0,327	0,091	GABA aminotransferase inhibitor

Pa: Probability of activity, Pi: Probability of inactivity.

Table 5: Adverse effects of phytomolecules from *A. rohituka*.

Sl. No.	Phytomolecules	Pa	Pi	Side effects
01.	Guaiol	0.356	0.226	Arrhythmia
02.	Alpha-Guaiene	0.344	0.239	Arrhythmia
03.	Beta-Sitosterol	0.258	0.205	Nephrotoxicity

Pa: Probability of activity, Pi: Probability of inactivity.

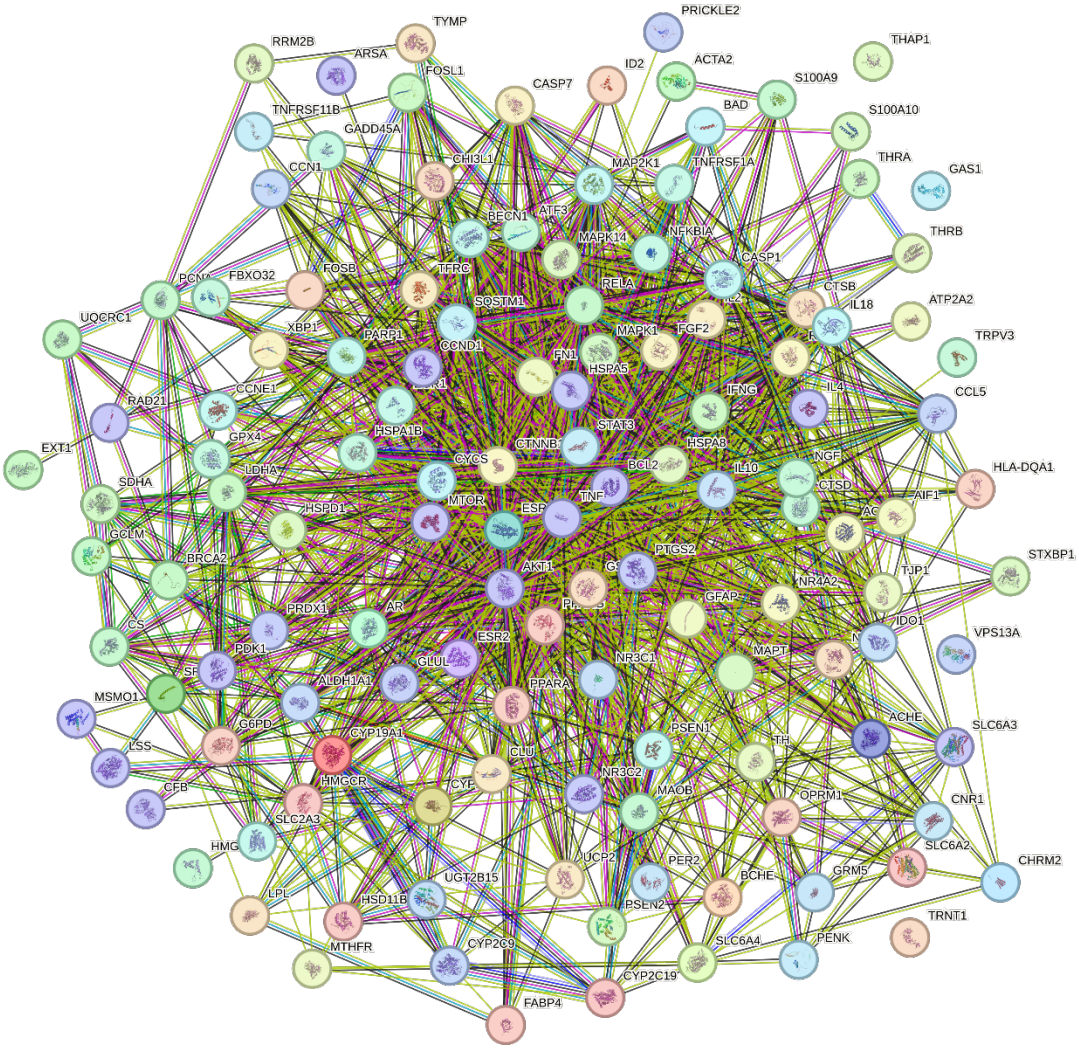

Figure 4: Protein-protein interaction of the genes modulated by the bioactives of *A. rohituka*.

of *A. rohituka*. Several additional pathways associated with depression were identified, including neurotrophin signalling, Tumour Necrosis Factor (TNF) signalling, Hypoxia-Inducible Factor-1 (HIF-1) signalling, Mechanistic Target of Rapamycin (mTOR) signalling, Forkhead box O (FoxO) signalling, Nuclear Factor Kappa B (NF-κB) signalling, Janus Kinase-Signal Transducer And Activator Of Transcription (JAK-STAT) signalling, cyclic AMP signalling, serotonergic synapse, dopaminergic synapse, glutamatergic synapse, and Adenosine Monophosphate-Activated Protein Kinase (AMPK) signalling. These pathways collectively regulate inflammatory responses, neurotransmitter homeostasis, oxidative stress, cellular metabolism, apoptosis, and neuroplasticity, all of which contribute to the pathogenesis of depression (Krishnan and Nestler, 2008; Castrén and Monteggia, 2021; Duman *et al.*, 2016). Hence the downregulation of these pathways and associated proteins are required for the management of depression. Gene Ontology analysis further supported the functional significance of the identified targets. The predominance of intracellular anatomical structures among cellular components indicates that most targets participate in intracellular signalling processes. Similarly, signalling receptor binding emerged as the principal molecular function, suggesting that many targets regulate receptor-mediated communication essential for neurotransmission and cellular signalling. The enrichment of regulation of multicellular organismal process as the most significant biological process further indicates involvement of these proteins in complex physiological functions including neuronal communication, immune regulation, and maintenance of central nervous system homeostasis (Ashburner *et al.*, 2000). Together, these findings complement the pathway analysis and reinforce the multitarget pharmacological profile predicted for *A. rohituka*. Molecular docking further validated the predicted interactions between the selected phytoconstituents and the identified protein targets. Bulnesol demonstrated the strongest docking affinity towards Estrogen Receptor 1 (ESR1) and Cytochrome P450 family 2 subfamily C member 19 (CYP2C19), while α-guaiene exhibited favourable binding with Peroxisome

Proliferator-Activated Receptor Alpha (PPARA), and himachalol interacted favourably with solute carrier family 6 member 4 (SLC6A4). The observed hydrogen bonds, polar interactions, and extensive hydrophobic contacts indicate stable accommodation of these ligands within the respective binding pockets (Meng *et al.*, 2011). Although the docking scores of several phytoconstituents were comparatively lower than those of the corresponding reference drugs, they nevertheless demonstrated favourable binding orientations and interactions with key amino acid residues involved in ligand recognition. Considering that herbal medicines generally exert therapeutic effects through the combined action of multiple phytochemicals acting on multiple molecular targets, these findings support the proposed multitarget mechanism of *A. rohituka* (Hopkins, 2008). The docking observations were further supported by MOLECULAR MECHANICS-GENERALIZED BORN SURFACE AREA (MM-GBSA) analysis, which estimates the binding free energy of ligand-protein complexes by incorporating molecular mechanics and solvation energy components. Bulnesol demonstrated favourable binding free energy values against several target

Table 6: KEGG pathways modulated by the bioactives of *A. rohituka*.

Sl. No.	Pathways	OGC	BGC	strength	signal	FDR	Matching proteins
01.	Neurotrophin signalling pathway	13	112	1.23	2.18	13	MAPK1, NFKBIA, MAPK14, NTRK2, MAP2K1, GSK3B, PSEN1, PSEN2, NGF, BAD, BCL2, RELA, AKT1
02.	PI3K-Akt signalling pathway	19	349	0.9	1.67	1.34E-10	MAPK1, IL2, CCND1, IL4, MDM2, CCNE1, FGF2, NTRK2, MAP2K1, GSK3B, FN1, MTOR, NGF, BAD, BCL2, RELA, CHRM2, PRKCA, AKT1
03.	HIF-1 signalling pathway	12	102	1.24	2.09	2.61E-10	MAPK1, IFNG, STAT3, MAP2K1, MTOR, TFRC, PDK1, BCL2, RELA, PRKCA, LDHA, AKT1
04.	TNF signalling pathway	11	111	1.16	1.78	6.49E-09	TNFRSF1A, MAPK1, NFKBIA, MAPK14, MAP2K1, PTGS2, CASP7, RELA, TNF, AKT1, CCL5
05.	MAPK signalling pathway	15	286	0.89	1.42	1.67E-08	TNFRSF1A, MAPK1, MAPK14, FGF2, NTRK2, MAP2K1, MAPT, NGF, GADD45A, HSPA1B, RELA, TNF, PRKCA, HSPA8, AKT1
06.	Autophagy - animal	11	131	1.09	1.62	2.60E-08	MAPK1, CTSD, MAP2K1, CTSL, CTSB, MTOR, BECN1, SQSTM1, BAD, BCL2, AKT1
07.	FoxO signaling pathway	10	126	1.07	1.46	1.85E-07	MAPK1, CCND1, MAPK14, MDM2, STAT3, MAP2K1, GADD45A, IL10, FBXO32, AKT1
08.	Serotonergic synapse	8	108	1.04	1.19	5.03E-06	MAPK1, CYP2C9, SLC6A4, MAP2K1, PTGS2, CYP2C19, MAOB, PRKCA
09.	JAK-STAT signalling pathway	9	158	0.92	1.09	8.23E-06	IL2, CCND1, IFNG, IL4, STAT3, MTOR, BCL2, IL10, AKT1
10.	mTOR signalling pathway	8	150	0.89	0.95	4.38E-05	TNFRSF1A, MAPK1, MAP2K1, GSK3B, MTOR, TNF, PRKCA, AKT1
11.	Dopaminergic synapse	7	126	0.91	0.89	0.00011	MAPK1, TH, SLC6A3, DRD2, MAOB, PRKCA, AKT1
12.	AMPK signalling pathway	5	120	0.79	0.57	0.0038	CCND1, PPARG, HMGCR, MTOR, AKT1
13.	Glutamatergic synapse	4	112	0.72	0.43	0.016	MAPK1, GRM5, GLUL, PRKCA
14.	NF-kappa B signalling pathway	8	101	1.07	1.24	3.33E-06	TNFRSF1A, NFKBIA, PARP1, PTGS2, GADD45A, BCL2, RELA, TNF
15.	cAMP signalling pathway	9	207	0.81	0.89	5.63E-05	MAPK1, NFKBIA, MAP2K1, GRM5, CHRM2, PRKCA, AKT1, CREB1, BDNF

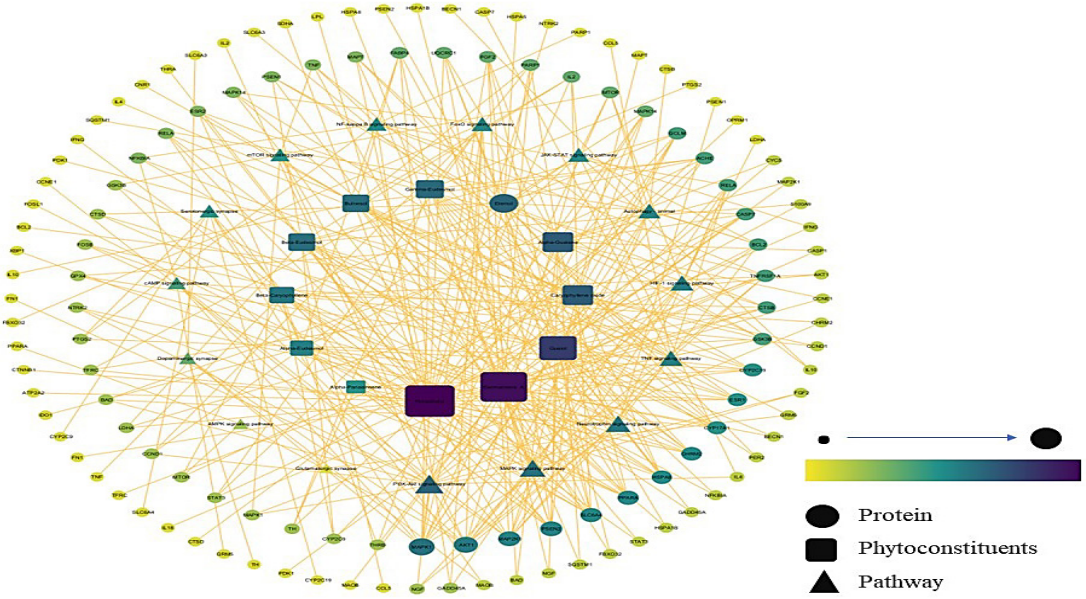

Figure 5: Network construction of bioactives from *A. rohituka,* their regulated targets, and modulated pathways.

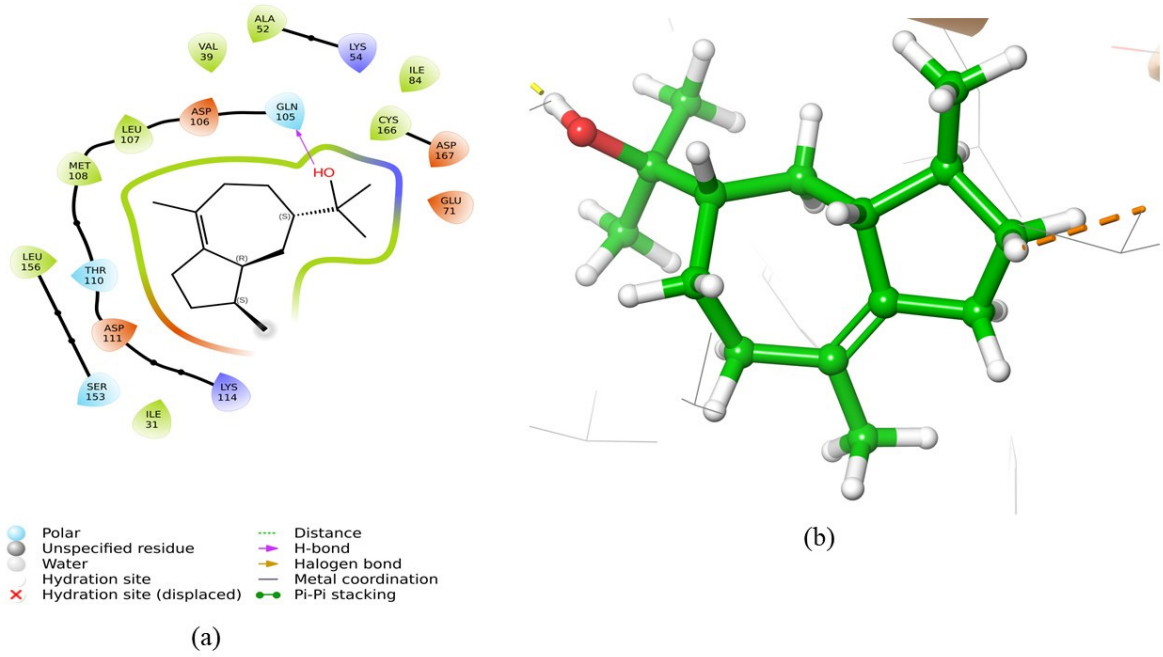

Figure 6: (a) 2D and (b) 3D interaction of bulnesol with ESR1 (1XPC).

proteins, particularly ESR1 and CYP2C19, whereas β-eudesmol also exhibited a favourable binding free energy against presenilin 2. The predominantly negative binding free energies indicate thermodynamically favourable complex formation, suggesting that these phytoconstituents are capable of forming stable protein-ligand interactions. Furthermore, the substantial contributions of van der Waals and lipophilic interaction energies indicate that hydrophobic interactions play a dominant role in stabilising these complexes, while Coulombic and solvation energy terms further contribute to binding affinity. Although several reference drugs exhibited stronger binding free energies, the observed MM-GBSA values of the phytoconstituents remain consistent with their predicted multitarget pharmacological behaviour. Overall, the present study demonstrates that *A. rohituka* possesses multiple phytoconstituents capable of interacting with several depression-associated proteins and signalling pathways. The integrated computational evidence suggests that its antidepressant potential may involve simultaneous regulation of PI3K-Akt, MAPK, neurotrophin, serotonergic, dopaminergic, mTOR, AMPK, NF-κB, TNF, and JAK-STAT signalling pathways, leading to improved neuroplasticity, modulation of neurotransmitter function, attenuation of

Table 7: Top binding energy of the bioactives and standard against respective proteins.

Compound	PDB ID	Docking score	Hydrophobic interactions	Polar interactions	Hydrogen bonds
Bulnesol	1XPC	-8.2	ILE31, LEU156, MET108, LEU107, VAL39, ALA52, ILE84, CYS166	SER153, THE110, GLN105	GLN105
Bulnesol	4GQS	-7.242	ALA106, ILE205, VAL208, ALA103, LEU102, PHE114, PHE100, VAL113, PHE476, LEU366, ALA297, ALA292, LEU201, MET240, LEU237, LEU233	ASN107, ASN 204	ASN107, ASN 204
α-guaine	2P54	-7.008	ALA250, ILE241, PHE343, LEU344, LEU247, ILE272, ILE339, CYS275, CYS276, MET330, VAL332, ALA333, LEU258, VAL255, LEU254	THR279	-
Himachalol	5I71	-6.98	TYR18, ILE19, PHE55	ASN53	GLU17
Bulnesol	3SWZ	-6.932	TYR201, ILE205, ILE206, VAL482, VAL483, LEU209, ALA105, PHE114, ALA113, TYR201,	SER106, ASN202	
Guaiol	1S9J	-6.276	MET219, ILE216, LEU215, LEU115, LEU118, VAL211, ILE141, PHE209, 1LE99	SER212, ASN192	PHE209
Bulnesol	1TV0	-5.746	ILE31, LEU156, MET108, LEU107, VAL39, ALA52, ILE84, CYS166	SER153, THR110, GLN105	GLN105
Bulnesol	3LDQ	-5.052	ILE343	SER275, SER340	GLU231, LYS271
Bulnesol	1UNQ	-4.049	LEU52, PHE55, TYR18	ASN54, ASN53, TYR18	LEU52, ASN53
B-eudesmol	7Y5X	-4.029	ALA700, ILE699, PHE698, ALA694	ASN691	PHE698
Tamoxifen	1XPC	-9.985	TRP383, LEU384, CYS530, LEU387, MET388, LEU391, PHE404, LEU402, LEU428, PHE425, ILE424, MET421, MET522, LEU525, TYR526, LEU346, LEU349, ALA350, MET343	THR347, HIE524	-
Doxepin	4GQS	-7.329	VAL113, VAL436, CYS435, ILE434, LEU366, ILE362, PHE428, LEU361, PRO427, ALA441, ALA297, PHE476	SER365, THR302, THR301	-
Fenofibrate	2P54	-8.814	MET355, ILE354, ILE317, PHE318, LEU321, MET330, VAL332, ALA333, ILE272, PHE273, ILE339, CYS275, CYS276, LEU460, LEU456, VAL444, TYR464, TYR314	GLN277, THR279, SER280, HIE440	-
Citalopram	5I71	-7.841	TYR176, TYR175, GLY442, LEU443, ALA173, ILE172, ALA169, PHE341, LEU337, TYR95, ALA96, LEU337, PHE335, VAL335, VAL501	SER439, SER438, ASN177, THR497	-
Ketoconazole	3SWZ	-8.965	ILE112, ALA113, PHE114, VAL483, ALA105, LEU243, ILE198, TYR201, ILE205, ILE206, PRO434, PHE435, LEU361, LEU209, VAL366, ALA367, LEU370, ILE371, CYS442, ILE443, ILE112, ALA113, PHE114, VAL483	ASN202, THR306, SER441	ARG239, CYS442

Compound	PDB ID	Docking score	Hydrophobic interactions	Polar interactions	Hydrogen bonds
Trametinib	1S9J	-7.709	ILE216, LEU215, MET230, MET219, ALA220, ILE99, ILE141, MET143, VAL127, CYS207, PHE209, VAL211, LEU115, LEU118	SER212, HIE188, ASN221	SER212, VAL211
Erlotinib	1TV0	-5.054	LEU156, MET108, LEU107, ALA52, ILE84, CYS166, VAL39, TYR36, ALA35	THR68, GLN105, THR110	ARG67
Acetaminophen	3LDQ	-5.120	TYR15	SER340	GLY339, GLU231, LYS271
Nirogastat	7Y5X	-1.975	ALA700, ILE699, PHE698, ALA694, ILE690	ASN691, THR687	PHE698
Fluvestrant	IUNQ	-3.444	PHE55, LEU52, ILE19, TYR18, ILE84	ASN54, ASN53, GLN79, THR82	TYR18, ILE19

Table 8: Binding free energy calculation of compounds with target proteins.

Compound code	PDB ID	MMGBSA dG Bind	MMGBSA dG Bind Coulomb	MMGBSA dG Bind Covalent	MMGBSA dG Bind Lipo	MMGBSA dG Bind Solv GB	MMGBSA dG Bind vdW
Bulnesol	1XPC	-42.18	-3.03	5.08	-25.07	13.58	-31.97
Bulnesol	4GQS	-43.66	-10.72	1.92	-19.35	14.41	-29.40
α-guaine	2P54	-34.37	-44.46	-1.77	-24.76	6.82	-20.69
Himachalol	5I71	-17.95	-8.93	2.10	-18.99	42.21	-33.80
Bulnesol	3SWZ	-31.41	-6.13	4.00	-19.33	18.97	-27.65
Guaiol	1S9J	-26.94	-7.84	4.60	-16.25	17.31	-24.18
Bulnesol	1TV0	-29.20	-8.40	1.35	-13.46	22.78	-30.71
Bulnesol	3LDQ	-22.35	-9.36	2.72	-10.71	20.44	-24.46
Bulnesol	1UNQ	-25.21	-21.22	0.47	-6.19	20.35	-17.59
B-eudesmol	7Y5X	-42.40	-14.84	3.19	-14.94	16.49	-30.33
Tamoxifen	1XPC	-70.98	-0.44	6.51	-44.09	31.48	-63.91
Doxepin	4GQS	-43.14	-8.31	1.75	-23.41	25.95	-38.64
Fenofibrate	2P54	-52.14	-8.62	14.79	-26.73	13.43	-44.31
Citalopram	5I71	-22.73	-2.83	3.10	-28.31	52.94	-46.11
Ketoconazole	3SWZ	-54.35	-14.76	8.17	-27.74	38.91	-57.52
Trametinib	1S9J	-79.22	-21.67	3.73	-26.15	32.12	-65.45
Erlotinib	1TV0	-33.87	-14.48	5.98	-15.87	32.43	-40.56
Acetaminophen	3LDQ	-24.24	-23.72	0.63	-4.22	23.16	-18.34
Nirogastat	1UNQ	-42.40	-14.84	3.19	-14.94	16.49	-30.33
Fluvestrant	7Y5X	-26.81	-35.09	4.71	-10.78	49.43	-31.77

dG Bind: binding free energy, Lipo: Lipophilic, Solv GB: Generalized Born Solvation Energy, vdW: van der Waals.

neuroinflammation, and enhanced neuronal survival (Castrén and Monteggia, 2021; Duman *et al.*, 2016). Nevertheless, the present findings are based exclusively on computational predictions, and therefore experimental validation through *in vitro, in vivo*, and clinical investigations is required to confirm the proposed molecular mechanisms and therapeutic efficacy. Despite these limitations, this study provides a comprehensive systems-level understanding of the antidepressant potential of *A. rohituka* and identifies several promising bioactive compounds that may serve as potential leads for future antidepressant drug discovery.

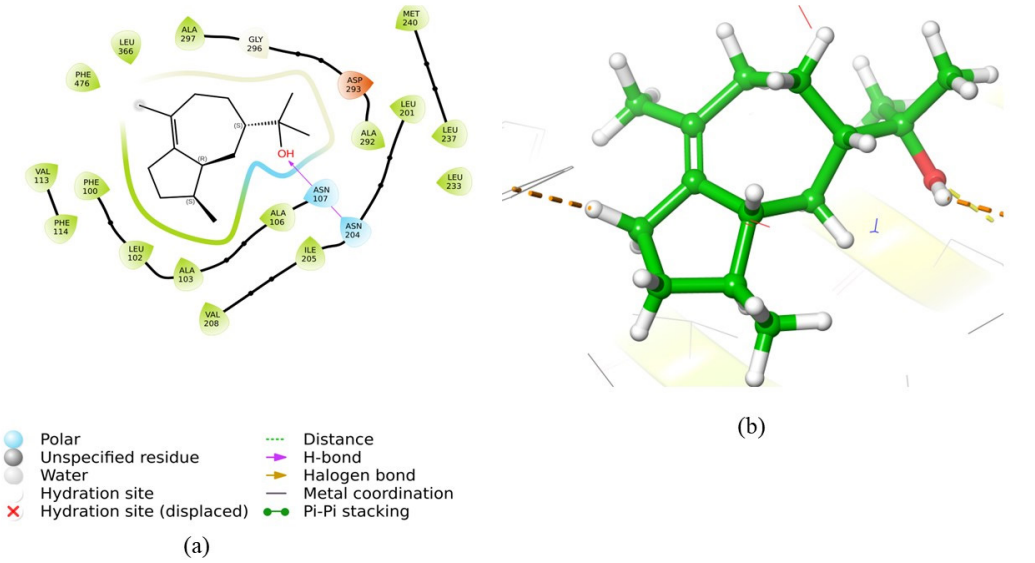

Figure 7: (a) 2D and (b) 3D interaction of bulnesol with CYP2C19 (4GQS).

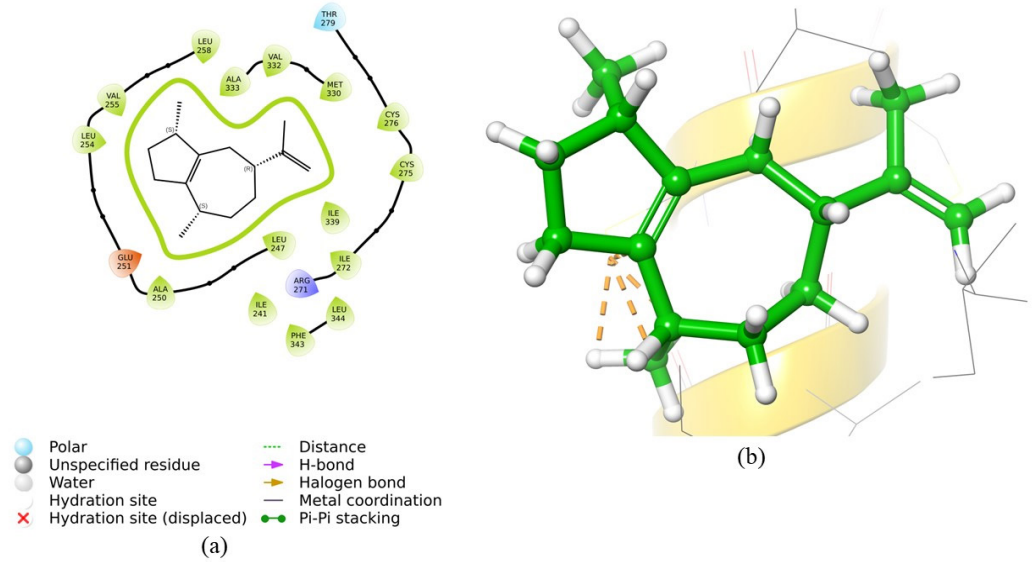

Figure 8: (a) 2D and (b) 3D interaction of α-guaine with PPARA (2P54).

CONCLUSION

The present study employed an integrated systems pharmacology approach to elucidate the potential molecular mechanisms underlying the antidepressant activity of *Amoora rohituka*. A total of 18 reported leaf phytoconstituents were identified, of which 12 satisfied the drug-likeness criteria and exhibited favourable pharmacokinetic characteristics for further evaluation. PASS prediction indicated that several phytoconstituents possess activities associated with neurotransmitter regulation, neuroprotection, anti-inflammatory signalling, and neuroplasticity. Network pharmacology identified 132 common targets between *A. rohituka* phytoconstituents and depression, with MAPK1, AKT1, PARP1, CDK2, and GSK3β emerging as key hub proteins. Functional enrichment analysis further demonstrated that the predicted targets were predominantly involved in PI3K-Akt, MAPK, neurotrophin, serotonergic synapse, dopaminergic synapse, mTOR, TNF, NF-κB, JAK-STAT, AMPK, and cAMP signalling pathways, highlighting the multitarget mechanism through which *A. rohituka* may exert antidepressant effects.Molecular docking demonstrated favourable binding of the selected phytoconstituents with several depression-associated proteins, with bulnesol exhibiting the strongest and broadest interaction profile, followed by α-guaiene, himachalol, guaiol, and β-eudesmol. The docking results were further supported by MM-GBSA analysis, which demonstrated favourable binding free energies and suggested the formation of stable ligand-protein complexes. Collectively, these findings

indicate that the antidepressant potential of *A. rohituka* is likely mediated through the coordinated modulation of multiple molecular targets and interconnected signalling pathways involved in neurotransmission, neuroplasticity, inflammation, oxidative stress, and neuronal survival. Overall, the present study integrates network pharmacology, PASS prediction, molecular docking, and MM-GBSA analysis to elucidate the antidepressant mechanism of *A. rohituka*. Although the findings provide valuable mechanistic insights and identify promising lead phytoconstituents for antidepressant drug discovery, they are based exclusively on computational predictions. Therefore, further validation through *in vitro* studies, *in vivo* experimental models, pharmacokinetic investigations, and clinical studies is required to confirm the proposed molecular mechanisms, therapeutic efficacy, and safety of *A. rohituka*.

ACKNOWLEDGEMENT

The authors are thankful to the authorities of Nitte (Deemed to be University) and Principal, NGSM Institute of Pharmaceutical Sciences, Mangaluru, for providing the laboratory facilities essential for the successful execution of this research work.

ABBREVIATIONS

ADR: Adverse Drug Reaction; **ADMET:** Absorption, Distribution, Metabolism, Excretion, and Toxicity; **AKT1:** AKT Serine/Threonine Kinase 1; **AMPK:** Adenosine Monophosphate-Activated Protein Kinase; **BBB:** Blood-Brain Barrier; **BCL2:** B-Cell Lymphoma 2; **BGC:** Background Gene Count; **BP:** Biological Process; **cAMP:** Cyclic Adenosine Monophosphate; **CC:** Cellular Component; **CDK2:** Cyclin-Dependent Kinase 2; **CTD:** Comparative Toxicogenomics Database; **CYP2C9:** Cytochrome P450 Family 2 Subfamily C Member 9; **CYP2C19:** Cytochrome P450 Family 2 Subfamily C Member 19; **DIGEP-Pred:** Drug-Induced Gene Expression Prediction; **DLS:** Drug-Likeness Score; **EGFR:** Epidermal Growth Factor Receptor; **ESR1:** Estrogen Receptor 1; **ESRRG:** Estrogen-Related Receptor Gamma; **FDR:** False Discovery Rate; **GO:** Gene Ontology; **GSK3β:** Glycogen Synthase Kinase-3 Beta; **HIF-1:** Hypoxia-Inducible Factor-1; **HSPA8:** Heat Shock Protein Family A Member 8; **IL:** Interleukin; **IMPPAT:** Indian Medicinal Plants, Phytochemistry and Therapeutics; **JAK2:** Janus Kinase 2; **JAK-STAT:** Janus Kinase-Signal Transducer and Activator of Transcription; **KEGG:** Kyoto Encyclopedia of Genes and Genomes; **MAP2K1:** Mitogen-Activated Protein Kinase Kinase 1; **MAPK:** Mitogen-Activated Protein Kinase; **MAPK1:** Mitogen-Activated Protein Kinase 1; **MAOB:** Monoamine Oxidase B; **MF:** Molecular Function; **MM-GBSA:** Molecular Mechanics Generalized Born Surface Area; **mTOR:** Mechanistic Target of Rapamycin; **MW:** Molecular Weight; **NF-κB:** Nuclear Factor Kappa B; **NFKBIA:** Nuclear Factor of Kappa Light Polypeptide Gene Enhancer in B-Cells Inhibitor Alpha; **NGF:** Nerve Growth Factor; **NHBA:** Number of Hydrogen Bond Acceptors; **NHBD:** Number of Hydrogen Bond Donors; **Nrf2:** Nuclear Factor Erythroid 2-Related Factor 2; **OGC:** Observed Gene Count; **OMIM:** Online Mendelian Inheritance in Man; **OPLS:** Optimized Potentials for Liquid Simulations; **Pa:** Probability of Activity; **PARP1:** Poly (ADP-Ribose) Polymerase 1; **PASS:** Prediction of Activity Spectra for Substances; **PDB:** Protein Data Bank; **Pi:** Probability of Inactivity; **PI3K:** Phosphoinositide 3-Kinase; **PPARA:** Peroxisome Proliferator-Activated Receptor Alpha; **PPI:** Protein-Protein Interaction; **PSEN2:** Presenilin 2; **PubChem CID:** PubChem Compound Identifier; **RMSD:** Root Mean Square Deviation; **SLC6A4:** Solute Carrier Family 6 Member 4; **SMILES:** Simplified Molecular Input Line Entry System; **STRING:** Search Tool for the Retrieval of Interacting Genes/Proteins; **SwissADME:** Swiss Absorption, Distribution, Metabolism, and Excretion; **TNF:** Tumour Necrosis Factor; **TTD:** Therapeutic Target Database; **UniProt:** Universal Protein Resource.

CONFLICT OF INTEREST

The authors declare that there is no conflict of interest.

AUTHOR CONTRIBUTION STATEMENT

Manjunatha Pai C: Set the hypothesis, performed the work, gathered and analysed data, and prepared the manuscript. **Rajesh K S:** Helped in hypothesis setup, supervised the work, interpretated data, helped in drafting and reviewing the manuscript. **Manappa T Mandalamari:** Helped in hypothesis setup, supervised the work, visualization, and reviewing the draft. **Abdul Fairoz Ahamed:** Helped in investigation, visualization, validation.

REFERENCES

Abraham, D. J., & Myers, M. (Eds.).(2021). Burger's medicinal chemistry, drug discovery and development (8th ed.). Wiley.

Ashburner, M., Ball, C. A., Blake, J. A., Botstein, D., Butler, H., *et al.* (2000). Gene ontology: Tool for the unification of biology. Nature Genetics, 25(1), 25-29. https://doi.org/10.1038/75556

Barabási, A.-L., Gulbahce, N., & Loscalzo, J. (2011). Network medicine: A network-based approach to human disease. Nature Reviews Genetics, 12(1), 56-68. https://doi.org/10.1038/nrg2918

Brigitta, B. (2002). Pathophysiology of depression and mechanisms of treatment. Dialogues in Clinical Neuroscience, 4(1), 7-20. https://doi.org/10.31887/DCNS.2002.4.1/bbondy

Cargnello, M., & Roux, P. P. (2011). Activation and function of the MAPKs and their substrates, the MAPK-activated protein kinases. Microbiology and Molecular Biology Reviews, 75(1), 50-83. https://doi.org/10.1128/MMBR.00031-10

Castrén, E., & Monteggia, L. M. (2021). Brain-derived neurotrophic factor signaling in depression and antidepressant action. Biological Psychiatry, 90(2), 128-136. https://doi.org/10.1016/j.biopsych.2021.05.008

Chaudhary, R. K., Karoli, S. S., Dwivedi, P. S., & Bhandari, R. (2022). Anti-diabetic potential of Corn silk (*Stigma maydis*): An *in silico* approach. Journal of Diabetes & Metabolic Disorders, 21(1), 445-454. https://doi.org/10.1007/s40200-022-00992-7

Chennaithody, S. (2025). Evaluation of Preliminary Phytochemical Screening, Estimation of Total Phenolic Content, and Antioxidant Potential of *Amoora rohituka* Roxb. Pharmacognosy Research, 18(1), 184-190. https://doi.org/10.5530/pres.20260042

Chennaithody, M. P., & Shankar, R. K. (2026). Antidepressant neuroprotective mechanisms of natural products in depression management: A comprehensive review. Pharmacognosy Research, 18(2), 224-236. https://doi.org/10.5530/pres.20260065

Duman, R. S., & Aghajanian, G. K. (2012). Synaptic dysfunction in depression: Potential therapeutic targets. Science, 338(6103), 68-72. https://doi.org/10.1126/science.1222939

Duric, V., Banasr, M., Licznerski, P., Schmidt, H. D., Stockmeier, C. A., *et al.* (2010). A negative regulator of MAP kinase causes depressive behavior. Nature Medicine, 16(11), 1328-1332. https://doi.org/10.1038/nm.2219

Dwivedi, P. S., Patil, R., Khanal, P., Gurav, N. S., *et al.* (2021a). Exploring the therapeutic mechanisms of *Cassia glauca* in diabetes mellitus through network pharmacology, molecular docking and molecular dynamics. RSC Advances, 11(62), 39362-39375. https://doi.org/10.1039/D1RA07661B

Dwivedi, P. S., Rasal, V. P., Kotharkar, E., Nare, S., & Khanal, P. (2021b). Gene set enrichment analysis of PPAR-γ regulators from *Murraya odorata* Blanco. Journal of Diabetes & Metabolic Disorders, 20(1), 369-375. https://doi.org/10.1007/s40200-021-00754-x

Dwivedi, P. S., & Shastry, C. S. (2023). System biology mediated assessment of molecular mechanism for sinapic acid against breast cancer: via network pharmacology and molecular dynamic simulation. Scientific Reports, 13(1), 21982. https://doi.org/10.1038/s41598-023-49178-z

Fathima, Z. C., James, J. P., & Tj, S. (2026). Molecular modelling and computational evaluation of functionalised isoxazoline as novel MAO inhibitors for Parkinson's disease. International Journal of Drug Delivery Technology, 16(26s), 281-295. https://doi.org/10.25258/ijddt.16.26s.29

Gumnick, J. F., & Nemeroff, C. B. (2000). Problems with currently available antidepressants. Journal of Clinical Psychiatry, 61(Suppl. 10), 5–15. https://pubmed.ncbi.nlm.nih.gov/10910012

Hopkins, A. L. (2008). Network pharmacology: The next paradigm in drug discovery. Nature Chemical Biology, 4(11), 682-690. https://doi.org/10.1038/nchembio.118

Hossain, M. S., Islam, M., Jahan, I., & Hasan, M. K. (2023). *Aphanamixis polystachya*: Pharmacological benefits, health benefits and other potential benefits. Phytomedicine Plus, 3(2), 100448. https://doi.org/10.1016/j.phyplu.2023.100448

Kitagishi, Y., Kobayashi, M., Kikuta, K., & Matsuda, S. (2012). Roles of PI3K/AKT/GSK3/mTOR pathway in cell signaling of mental illnesses. Depression Research and Treatment, 2012(1), 752563.

Krishnan, V., & Nestler, E. J. (2008). The molecular neurobiology of depression. Nature, 455(7215), 894-902. https://doi.org/10.1038/nature07455

Kumar, K. S., Srivastava, S., Paswan, S., & Dutta, A. S. (2012). Depression-symptoms, causes, medications and therapies. The Pharma Innovation, 1(3, Part A), 37.

Meng, X.-Y., Zhang, H.-X., Mezei, M., & Cui, M. (2011). Molecular docking: A powerful approach for structure-based drug discovery. Current Computer-Aided Drug Design, 7(2), 146-157. https://doi.org/10.2174/157340911795677602

Stringaris, A. (2017). What is depression? Journal of Child Psychology and Psychiatry, 58(12), 1287–1289. https://doi.org/10.1111/jcpp.12844

Thomas, G. M., & Huganir, R. L. (2004). MAPK cascade signalling and synaptic plasticity. Nature Reviews Neuroscience, 5(3), 173-183. https://doi.org/10.1038/nrn1346.

Cite this article: Chennaithody MP, Shankar RK, Mandalamari MT, Ahamed AF. Network Pharmacology and Molecular Docking Analysis of *Amoora rohituka* Roxb. Reveals Bulnesol Modulates ESR1 and CYP2C19 Proteins as Potential Therapeutic Targets for Neuroprotection in the Management of Depression. J Young Pharm. 2026;18(3):816-32.